Contributions of extravascular and intravascular cells to fibrin network formation, structure, and stability

Robert A. Campbell, Katherine A. Overmyer, Craig H. Selzman, Brett C. Sheridan and Alisa S. Wolberg

Updated information and services can be found at:
http://bloodjournal.hematologylibrary.org/cgi/content/full/114/23/4886

Articles on similar topics may be found in the following *Blood* collections:
Thrombosis and Hemostasis (274 articles)
Vascular Biology (211 articles)

Information about reproducing this article in parts or in its entirety may be found online at:
http://bloodjournal.hematologylibrary.org/misc/rights.dtl#repub_requests

Information about ordering reprints may be found online at:
http://bloodjournal.hematologylibrary.org/misc/rights.dtl#reprints

Information about subscriptions and ASH membership may be found online at:
http://bloodjournal.hematologylibrary.org/subscriptions/index.dtl

Contributions of extravascular and intravascular cells to fibrin network formation, structure, and stability

Robert A. Campbell,[1] Katherine A. Overmyer,[1] Craig H. Selzman,[2] Brett C. Sheridan,[2] and Alisa S. Wolberg[1]

[1]Department of Pathology and Laboratory Medicine, and [2]Division of Cardiothoracic Surgery, Department of Surgery, University of North Carolina, Chapel Hill

Fibrin is essential for hemostasis; however, abnormal fibrin formation is hypothesized to increase thrombotic risk. We previously showed that in situ thrombin generation on a cell's surface modulates the 3-dimensional structure and stability of the fibrin network. Currently, we compared the abilities of extravascular and intravascular cells to support fibrin formation, structure, and stability. Extravascular cells (fibroblasts, smooth muscle) supported formation of dense fibrin networks that resisted fibrinolysis, whereas unstimulated intravascular (endothelial) cells produced coarse networks that were susceptible to fibrinolysis. All 3 cell types produced a fibrin structural gradient, with a denser network near, versus distal to, the cell surface. Although fibrin structure depended on cellular procoagulant activity, it did not reflect interactions between integrins and fibrin. These findings contrasted with those on platelets, which influenced fibrin structure via interactions between β3 integrins and fibrin. Inflammatory cytokines that induced pro-thrombotic activity on endothelial cells caused the production of abnormally dense fibrin networks that resisted fibrinolysis. Blocking tissue factor activity significantly reduced the density and stability of fibrin networks produced by cytokine-stimulated endothelial cells. Together, these findings indicate fibrin structure and stability reflect the procoagulant phenotype of the endogenous cells, and suggest abnormal fibrin structure is a novel link between inflammation and thrombosis. (Blood. 2009;114:4886-4896)

Introduction

Fibrin network production is essential for hemostasis, and an increasing number of studies implicate abnormal fibrin structure and stability in thrombotic disease, including premature myocardial infarction, and venous thromboembolism.[1,2] Fibrin production is the culmination of procoagulant processes that generate thrombin at an injury site. These processes are initiated by exposure of extravascular tissue factor (TF)–bearing cells after vascular disruption (hemostasis), or triggered by inappropriate expression of intravascular procoagulant activity (thrombosis). Understanding cellular and biochemical mechanisms contributing to fibrin formation, structure, and stability is fundamental for continued development of antithrombotic and thrombolytic therapies.

Previous studies have shown the thrombin concentration catalyzing the conversion of fibrinogen to fibrin influences fibrin structure and stability. Low thrombin concentrations produce coarse fibrin networks that are relatively susceptible to fibrinolysis, whereas high thrombin concentrations produce dense networks that resist fibrinolysis.[3-7] These differences in fibrinolytic susceptibility have significant physiologic implications: clots that are susceptible to fibrinolysis are prone to premature lysis and bleeding, whereas clots that resist fibrinolysis are prone to thrombosis.[8]

Although the role of thrombin in fibrin formation has been heavily scrutinized, few studies have examined the contributions of cells—the site of thrombin generation—to fibrin formation, structure, and stability. We previously demonstrated that in situ thrombin generation on the cell surface modulates the 3-dimensional structure and stability of the fibrin network. When thrombin generation is localized to a cell surface, clots develop a significantly denser fiber network within 10 micrometers of the surface compared with distal regions of the clot (40-50 micrometers from the cell surface).[9] Notably, the proximal, dense fibrin network is resistant to lysis compared with the distal, coarse network, suggesting the clot's structural heterogeneity dictates its fibrinolytic susceptibility.[9] Together, these findings suggest that when thrombin generation is localized to a cell surface, the fibrin network reflects its spatial location and the procoagulant phenotype of the local cell population.[9]

A cell's ability to support thrombin generation is determined by its expression of procoagulant and anticoagulant activities. For example, TF expression initiates thrombin generation, and phosphatidylserine exposure is necessary for robust thrombin generation through prothrombinase activity.[10] Tissue factor pathway inhibitor and thrombomodulin down-regulate thrombin generation by negatively regulating TF and factors V and VIII activity, respectively.[11,12] Because expression of these properties is cell specific, cells from different vascular locations differ in their ability to support thrombin generation.[13] Extravascular cells (fibroblasts and smooth muscle cells [SMCs]) are highly procoagulant and primed to support hemostasis, whereas intravascular (endothelial) cells suppress thrombin generation and fibrin formation.[14,15] However, exposure of intravascular cells to bacterial lipopolysaccharide,[16] hypoxia,[17] or inflammatory cytokines[18] induces expression of a procoagulant/prothrombotic phenotype. Although prior studies have compared thrombin generation on these cells, the contributions of these cells toward clot structure and stability have not previously been investigated.

In the current study, we compared the abilities of extravascular and intravascular cells to modulate fibrin formation, structure, and

stability. Our findings show that procoagulant extravascular cells (fibroblasts, SMCs) supported the formation of dense fibrin networks that resisted fibrinolysis. Network structure depended on procoagulant activity but not interactions between integrins and fibrin. Inflammatory cytokines induced prothrombotic activity on endothelial cells and subsequent production of an abnormally stable fibrin network. Blocking TF reduced fibrin network density and stability of clots produced by cytokine-stimulated intravascular cells. These findings suggest fibrin network formation, structure, and stability are important determinants of hemostasis and vascular cell–specific thrombosis.

Methods

Protein and materials

Sources of proteins and materials are provided in supplemental Materials (available on the *Blood* website; see the Supplemental Materials link at the top of the online article). Human blood and vessel segments were obtained through the University of North Carolina at Chapel Hill with institutional review board approval.

Cell culture

Immortalized human fibroblasts (NHF$_1$-hTert), generously provided by Dr Marila Cordeiro-Stone (University of North Carolina at Chapel Hill), were grown as described.[9,19] Primary human umbilical vein endothelial cells (HUVECs) pooled from 3 donors and aortic smooth muscle cells (SMCs) from 1 donor were from Lonza Walkersville and cultured as directed by Lonza. Cells were used between passages 3 to 10 to reduce phenotypic drift. Cells (7500/well) were seeded in 96-well tissue culture flat-bottom plates, grown to 80% to 95% confluence, and washed with phosphate-buffered saline (PBS) before use.

TF, prothrombinase activity, and activated protein C generation assays

TF (Xa generation), prothrombinase activity (thrombin generation), and activated protein C generation were measured by chromogenic substrate cleavage on a SpectraMax 340PC plate reader (Molecular Devices), as described.[9,12,20]

Determination of protein expression by Western blot analysis

Proteins (40 μg) were separated by 4% to 12% sodium dodecyl sulfate–polyacrylamide gel electrophoresis and transferred to NitroBind Pure Nitrocellulose (GE Osmonics). Western blotting for expression of thrombomodulin and integrin subunits αv and β3 was performed as described, using extracellular signal-related kinase 2 as a loading control.[21] Proteins were visualized with an enhanced chemiluminescence detection kit (Amersham Biosciences).

Normal pooled plasma preparation

Blood was collected from 30 healthy subjects (53% female, 40% nonwhite) through a 21-gauge butterfly into a syringe. The first 5 mL was used to prepare platelet-poor plasma and measure partial thromboplastin times for each donor. The following 30 mL was drawn into a separate syringe and immediately transferred to sodium citrate/corn trypsin inhibitor (CTI; 0.105 M/3.2% sodium citrate, pH 6.5, 18.3 μg/mL CTI) to minimize contact activation.[22] Platelet-free plasma (PFP) was prepared by sequential centrifugation (150g for 15 minutes, 13000g for 15 minutes), aliquoted, and snap-frozen in liquid nitrogen within 2 hours of blood collection. Normal pooled PFP was prepared by pooling PFP from persons with normal partial thromboplastin times. PFP was analyzed for activity levels of factors V, VII, VIII, IX, X, and XI, protein C, free protein S, and fibrinogen at University of North Carolina Hospitals McLendon Clinical Laboratory; all were in the normal reference range.

Thrombin generation in normal pooled plasma

Thrombin generation was measured by calibrated automated thrombography using a Fluoroskan Ascent fluorometer (ThermoLabsystem), as described[23-25] except 80 μL of PFP and 20 μL of HEPES-buffered saline/bovine serum albumin were added to washed cell monolayers to initiate reactions (67.7% plasma, final). Addition of fluorogenic substrate, alone, to cell monolayers did not produce signal, indicating the cell types did not express endogenous substrate cleaving activity (data not shown).

Thrombin generation was calculated using Thrombinoscope software Version 3.0.0.29 (Thrombinoscope BV). The thrombin generation rate was calculated by dividing the peak height by the difference from time to peak to lag time. The endogenous thrombin potential was not reported because thrombin generation curves on unstimulated HUVECs did not return to baseline.

Clot formation and lysis assays

Clotting was initiated by incubating cells with recalcified (10mM, final) normal, pooled PFP (86.7% plasma, final). In some assays, fibrinogen (2 mg/mL), CaCl$_2$ (5mM, final), and thrombin (2nM, final) were added to cells instead of plasma to examine networks formed in the absence of in situ thrombin generation. Exogenous thrombin addition to unstimulated and stimulated HUVECs caused cells to lose their normal polygonal shape due to actin polymerization.[26] To prevent actin polymerization and cell contraction, confluent HUVECs were treated for 30 minutes with the Rho-associated kinase inhibitor Y-27632 (10μM, final) in culture media; this inhibitor does not prevent fibrin from interacting with β3 integrins.[27] Fibrinolysis assays were performed by adding tissue plasminogen activator (tPA; 250 ng/mL, final) to PFP at the reaction start. Clot formation and lysis were detected by turbidity at 405 nm in a SpectraMax 340PC plate reader.

Clotting on platelet monolayers was performed by adhering gel-filtered platelets[28] (10^6 total) to collagen-coated (50 μg/mL, final) glass coverslips and activating platelets with SFLLRN (50 μg/mL, final) in the presence of abciximab or control immunoglobulin G (IgG; 0.136μM, final) and MgCl$_2$ (2mM final). Platelets were allowed to adhere and activate for 30 minutes at 37°C before coverslips were washed with HEPES-buffered saline/bovine serum albumin to remove nonadherent platelets. Recalcified (10mM, final), normal PFP with abciximab or control IgG and lipidated TF (Innovin; 1:120 000, final) was then added to platelets. Clots were allowed to form for 2 hours before imaging.

Structural analysis by laser scanning confocal microscopy

Cells (33 000/well) were seeded in Lab-Tek II Chamber no. 1.5 coverglass (Nalge Nunc International) and grown to 80% to 95% confluence. Clots were formed as for clotting assays with the addition of AlexaFluor-488–labeled fibrinogen (10 μg/150 μL sample, 3.2% of total fibrinogen). Synthetic peptide GRGDSP (500μM, final), which blocks binding to RGD-mediated receptors, or control peptide GRGESP was included as indicated. Clotting proceeded until a constant final turbidity was reached in separate, parallel reactions monitored in a SpectraMax 340PC plate reader.

Clots were imaged at room temperature as described[9] on a Zeiss LSM5 Pascal laser scanning confocal microscope linked to a Zeiss Axiovert 200M microscope equipped with a Zeiss 63×/1.4 NA oil-immersion plan apo-chromatic lens. The 488-nm line of a medium power multiline argon ion laser was used for excitation and a 505- to 530-nm band-pass filter for emission. A computer equipped with Carl Zeiss software (v1.5) was used to operate the system. Optical sectioning was achieved by closing the pinhole in the front of the detector to 1 airy unit. The zoom factor was 1. Thirty optical sections (1024 × 1024 pixels each) in 3 randomly chosen locations were collected at 0.36-μm intervals in the z-axis at the cell surface (defined as when the cells were in focus using differential interference contrast microscopy) and 40 μm above the cell surface, thus covering a region 10.8 μm thick at and above the cell surface. Image volumes were 146 × 146 × 10 μm. Single images were collected in 15.47 seconds. Optical resolution was approximately 0.14 μm in the xy-plane and approximately 0.5 μm on the z-axis. The sectioning interval in z was smaller than the calculated z-axis optical section resolution to achieve Nyquest sampling in z based on the Zeiss software calculation. No correction was made for refractive index mismatch. Images were deconvolved using 3-dimensional

deconvolution algorithms in AutoQuant's Autodeblur (Version x1.4.1; Media Cybernetics Inc). Fibrin network density was analyzed using ImageJ (1.37V; National Institutes of Health) by placing random grids of 2 pixel crosses on individual slices (~ 121-144 crosses/slice), and counting fibers intersecting the middle of the crosses, divided by the total number of crosses. In slices near the cell surface, crosses placed over cells (indicated by "empty" space) were subtracted from the total number of crosses to correct for the volume occupied by the cell.[9] Optical resolution (0.14 µm [xy] by 0.5 µm [z]) was near the lower limit of resolution to measure fibrin fiber diameter accurately; therefore, fibrin diameter analysis was not performed.[3]

Structural analysis of ex vivo clots by transmission electron microscopy

Saphenous vein segments (2-6 cm) were obtained with informed consent from patients undergoing coronary artery bypass grafting under a protocol approved by the University of North Carolina institutional review board. After removal, vein segments were placed in heparinized saline before immediate transfer to the laboratory where they were placed into PBS and cut longitudinally down the midline, creating 2 vessel halves. Vessel segments were then cut laterally and placed into individual chambers on a permanox slide, lumen side up. Vessels were then washed 5 times with PBS, and recalcified (10mM, final) plasma was added to the vessel lumen. After 2 hours, clots were fixed overnight in 4% paraformaldehyde/1% glutaraldehyde in PBS. Fixed clots were washed and embedded in Epon for thin sectioning. Clots were imaged using a LEO EM910 transmission electron microscope (Carl Zeiss SMT) operating at 80 kV. Digital images were recorded using a Gatan Orius CCD Digital Camera and Digital Micrograph 3.11.0 (Gatan Inc). Fibrin density was determined on 6300× micrographs by placing 1-µm-thick boxes parallel to, and 0.25 µm and 5 µm from, the cell surface and counting fibers inside the box.[9]

Statistical methods

Continuous variables were expressed as mean plus or minus SD. Pairwise comparisons were performed by Student *t* test. A 1-way analysis of variance with Dunnett posthoc test using unstimulated HUVECs as the index group was used to control for error of multiple testing. *P* values less than .05 were considered significant.

Results

Extravascular cells enhance thrombin generation and fibrin formation compared with intravascular cells

We first compared the abilities of extravascular cells (fibroblasts, SMCs) and intravascular cells (HUVECs) to support thrombin generation and fibrin formation in recalcified, contact-inhibited PFP. As in previous studies,[15,29] thrombin generation on fibroblasts and SMCs demonstrated a significantly shorter lag time, higher rate, shorter time to peak, and increased peak height than on unstimulated HUVECs (Figure 1A, Table 1). Although the final peak turbidities of all clots were similar, fibroblasts and SMCs supported a significantly faster onset and rate of clot formation than unstimulated HUVECs (Figure 1B, Table 1).

Proinflammatory cytokines (TNFα) induce HUVEC procoagulant activity and increase fibrin formation

To determine how inflammatory cytokines influence fibrin formation and stability, we first treated HUVECs with 0 to 1nM tumor necrosis factor-α (TNFα) for 4 hours. Consistent with previous findings,[18,30] TF activity (factor Xa generation) was dose dependent with respect to TNFα concentration (Figure 1A inset). Subsequent assays were performed with HUVECs treated with 1nM TNFα for 4 hours. We first examined thrombin generation and fibrin forma-
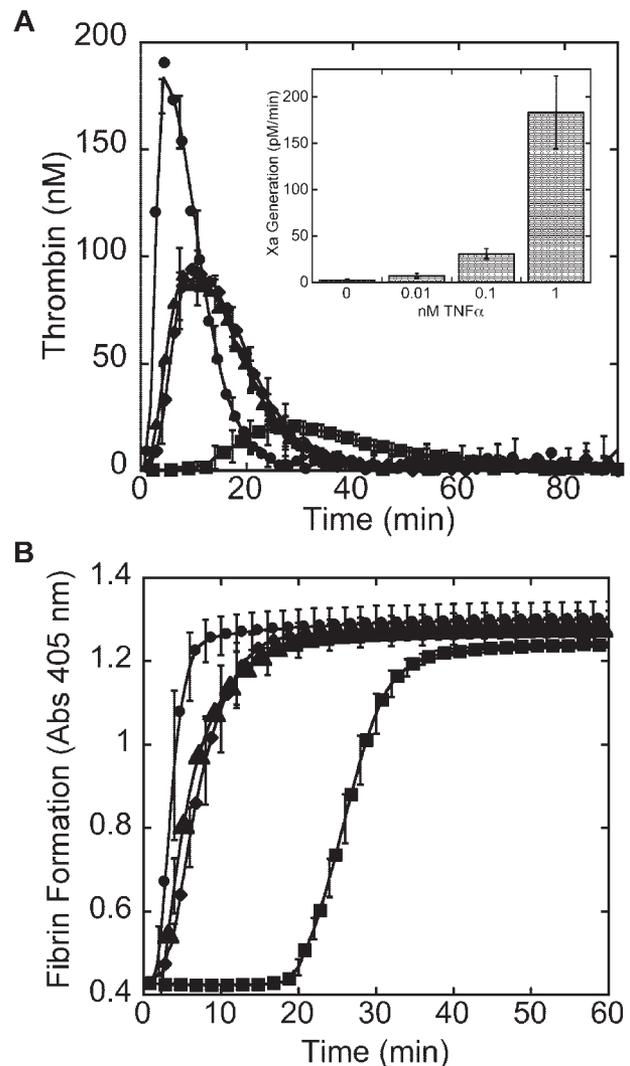

Figure 1. Extravascular and intravascular cells support different levels of thrombin generation and fibrin formation. Recalcified (10mM, final) normal, pooled PFP was added to confluent cell monolayers. (A) Thrombin generation was measured using calibrated automated thrombography; data (± SD) shown are averaged from at least 5 separate experiments. (A inset) HUVECs were incubated with TNFα (0-1nM) for 4 hours at 37°C. Factor Xa generation (± SD) was measured by incubating cells with factors VIIa and X in the presence of CaCl₂, and measuring factor Xa generation by chromogenic substrate in 2 separate experiments. (B) Fibrin polymerization was measured by turbidity at 405 nm; data (± SD) shown are from 1 experiment, representative of at least 7 independent experiments. Symbols for panels A and B are as follows: fibroblasts, (●); SMCs, (♦); HUVECs, (■); and HUVECs stimulated with TNFα for 4 hours, (▲).

tion, structure, and stability. Compared with unstimulated HUVECs, TNFα-stimulated HUVECs exhibited a significantly shorter lag time and time to peak, and increased rate and peak height of thrombin generation (Figure 1A, Table 1). Compared with unstimulated HUVECs, TNFα stimulation also significantly shortened the onset and increased the rate of clot formation (Figure 1B, Table 1). We observed similar findings with interleukin-1β (IL-1β)–stimulated cells (data not shown). In short, cytokine stimulation increased HUVEC procoagulant activity to a level similar to that of extravascular cells (SMCs).

Different vascular cells produce different fibrin network structures

We next incubated fibroblast, SMC, and unstimulated and TNFα-stimulated HUVEC monolayers with recalcified, normal pooled

Table 1. Thrombin generation and fibrin formation supported by fibroblasts, SMCs, HUVECs, and TNFα-stimulated HUVECs

			HUVECs	
	Fibroblasts	**SMCs**	**Unstimulated**	**+ TNFα**
Thrombin generation				
Lag time, min	1.7 ± 0.2*	3.6 ± 0.6*	12.8 ± 1.8	2.4 ± 0.2*
Rate, nM/min	60.5 ± 4.0*	14.9 ± 1.9*	1.5 ± 0.4	14.3 ± 4.0*
Time to peak, min	4.8 ± 0.3*	10.1 ± 1.0*	27.6 ± 3.0	9.0 ± 0.8*
Peak height, nM	189.1 ± 8.1*	95.6 ± 6.6*	22.4 ± 6.4	91.4 ± 13.8*
Clot formation				
Clotting onset, min	1.9 ± 0.6*	2.5 ± 0.4*	22.6 ± 7.7	2.1 ± 0.7*
Fibrin polymerization rate, mOD/min	238.5 ± 58.3*	138.4 ± 18.5*	56.5 ± 28.9	109.5 ± 34.4*
Final turbidity at 405 nm	0.822 ± 0.030	0.842 ± 0.020	0.787 ± 0.040	0.830 ± 0.060

SMC indicates smooth muscle cell; HUVEC, human umbilical vein endothelial cell; TNFα, tumor necrosis factor-α; and mOD, milli-optical density unit.

*P value less than .05 versus unstimulated HUVECs.

PFP and used laser scanning confocal microscopy to examine the fibrin structure of clots produced by these cells. Consistent with thrombin generation and fibrin formation measurements, clots produced by fibroblasts and SMCs were composed of densely and moderately packed networks, respectively, whereas clots produced by unstimulated HUVECs were composed of an open, coarse network (Figure 2A-C,E-G, Table 2). TNFα-stimulated (Figure 2D,H) and IL-1β–stimulated (data not shown) HUVECs produced significantly denser networks than unstimulated HUVECs, more like those produced by SMCs. Together, these findings show extravascular cells (fibroblasts, SMCs) produce denser fibrin networks than unstimulated intravascular (endothelial) cells, but stimulating endothelial cells with proinflammatory cytokines in-

duces their adoption of an extravascular cell–like prothrombotic phenotype that produces an abnormally dense fibrin network (Table 2).

In situ thrombin generation is necessary and sufficient to dictate the fibrin density gradient in clots produced by fibroblasts, SMCs, and HUVECs

In addition to individual effects of cells on network density, our analysis also showed clots produced by cultured fibroblasts, SMCs, and HUVECs demonstrated increased fibrin density near (0-10 μm) versus distal (> 10 μm) to the cell surface (Figure 2 compare A, B, C, and D with E, F, G, and H, respectively, 2M, Table 2, and Campbell et al[9]). We confirmed these findings in clots produced by
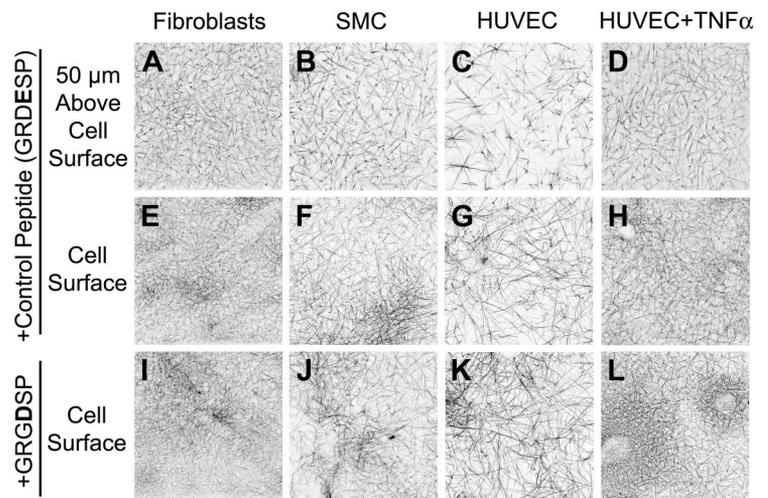

Figure 2. In situ thrombin generation on the cell surface modulates clot architecture in 3 dimensions. Clots were formed by incubating cells with recalcified normal, pooled PFP in the presence of 500μM (final) control peptide GRGESP (A-H) or GRGDSP (I-L). Three-dimensional projections show clot architecture in 10-μm stacks at (E-L) and above (A-D) the cell surface. Each image (146 μm × 146 μm, xy) is from 1 experiment, representative of at least 3 independent experiments. Darker areas show increased fibrin density. (M) Fibrin network density (± SD) of clots produced by fibroblasts (●), SMCs (♦), HUVECs (■), and TNFα-stimulated HUVECs (▲) was determined as described in "Methods" from at least 3 independent experiments. (N) Clots were formed in excised human saphenous vein segments as described in "Structural analysis of ex vivo clots by transmission electron microscopy." Clots were then fixed, examined by transmission electron microscopy, and fibrin fibers (black dots) were quantified at (0 μm) and above (5 μm) from the cell surface (indicated by black rectangles). Original magnification, × 2000; bar represents 5 μm. The image is representative of 3 independent experiments.
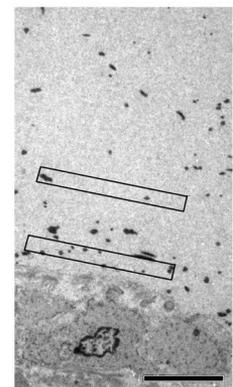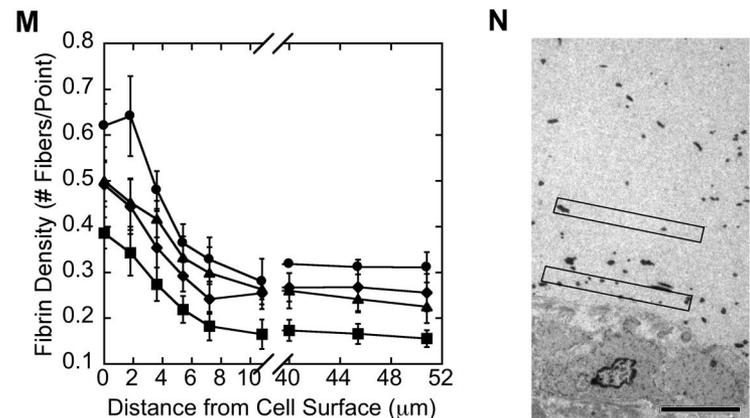
Table 2. Fibrin network density in clots formed by in situ thrombin generation on fibroblasts, SMCs, HUVECs, and TNFα-stimulated HUVECs

	Fibrin network density		P, 0-10 μm versus 40-50 μm
	0-10 μm	40-50 μm	
Fibroblasts			
+ Control peptide	0.796 ± 0.035	0.515 ± 0.045	.001
+ GRGDSP	0.835 ± 0.012	0.527 ± 0.054	.016
P, ± GRGDSP	NS	NS	
SMCs			
+ Control peptide	0.683 ± 0.034	0.455 ± 0.062	.001
+ GRGDSP	0.666 ± 0.058	0.446 ± 0.001	.003
P, ± GRGDSP	NS	NS	
HUVECs			
+ Control peptide	0.546 ± 0.053	0.306 ± 0.050	.001
+ GRGDSP	0.579 ± 0.114	0.364 ± 0.020	.03
P, ± GRGDSP	NS	NS	
HUVECs + TNFα			
+ Control peptide	0.723 ± 0.037	0.468 ± 0.011	.001
+ GRGDSP	0.730 ± 0.005	0.475 ± 0.059	.026
P, ± GRGDSP	NS	NS	

SMC indicates smooth muscle cell; HUVEC, human umbilical vein endothelial cell; TNFα, tumor necrosis factor-α; and NS, not significantly different with control (GRDESP) or β3-blocking (GRDGSP) peptide.

freshly excised human blood vessels, by adding recalcified, normal PFP to the lumen of excised, washed, saphenous veins isolated from patients undergoing coronary bypass surgery. Clots formed in vessels for at least 2 hours before fixation, thin sectioning, and imaging in cross-section by transmission electron microscopy. Similar to our in vitro findings with cultured cells (Figure 2A-M and Campbell et al[9]), clots produced in vessels ex vivo showed significantly ($P = .007$) increased fibrin density near versus distal to the vessel wall (1.23 ± 0.08 vs 0.57 ± 0.20 fibers/μm[2], respectively; Figure 2N). These findings confirm that the observed fibrin density gradient is not an artifact of cultured cells, but is also likely to arise from procoagulant activity expressed by cells within the vasculature.

We previously showed fibroblasts produce this fibrin density gradient via thrombin diffusion from the site of generation on the cell surface.[9] However, other studies have shown cellular integrins, specifically αIIbβ3 and αvβ3, increase fibrin network density and organization on platelets[31] and HUVECs,[32] respectively. Those studies were performed by adding exogenous thrombin to plasma[31] or fibrinogen[32] in the presence of cells. Thus, although both SMCs and HUVECs express αv and β3 subunits[32-34] (data not shown), the relative roles of in situ thrombin generation and integrin interac-

tions in dictating fibrin structure in plasma clots have not been established for SMCs or HUVECs.

To investigate the role of integrins in determining fibrin structure on these cells, we formed clots via in situ thrombin generation in the presence of 500μM GRGDSP peptide or GRGESP control peptide. This concentration of GRGDSP fully inhibits RGD-mediated interactions[32,35] and blocks platelet aggregation (data not shown), but does not alter the rates of thrombin generation or fibrin polymerization in plasma (data not shown). Fibrin density produced by fibroblasts, SMCs, or HUVECs was not altered by GRGDSP peptide (Figure 2 compare E, F, G, and H with I, J, K, and L, respectively, Table 2, supplemental Figure 1). Clinically relevant concentrations of anti-β3 integrin abciximab (0.136μM)[31] similarly failed to reduce network density (Figure 3), indicating the lack of involvement of integrins in determining network structure on these cells.

To evaluate the role of in situ thrombin generation in fibrin network production, we triggered clotting on fibroblasts, SMCs, and HUVECs via exogenous thrombin addition to purified fibrinogen. These reactions bypass in situ thrombin generation, and fibrin formation occurs within a uniform thrombin concentration. Under these conditions, fibroblasts, SMCs, and HUVECs did not produce a fibrin density gradient like that seen during in situ thrombin generation, and GRGDSP peptide did not decrease fibrin density in these clots (supplemental Figure 2, supplemental Table 3). These results confirm the central role of cellular procoagulant activity in determining the 3-dimensional network structure on fibroblasts, SMCs, and HUVECs.

In contrast to fibroblasts, SMCs, and HUVECs, platelets increase fibrin density via β3 integrins

Because previous studies have shown a significant influence of β3 integrins on platelets,[31] we compared findings with fibroblasts, SMCs, and HUVECs with those with platelets. Clots were formed on platelets via in situ thrombin generation (plasma plus soluble TF) or exogenous thrombin addition (fibrinogen plus thrombin) in the absence or presence of abciximab. Under these conditions, the thrombin generation rate did not change in the absence or presence of abciximab and was similar to HUVECs (data not shown). Figure 4 shows patches of increased fibrin density in clots produced by in situ thrombin generation (Figure 4A,C), likely reflecting contributions of platelet procoagulant surface in these reactions. Reactions with exogenous thrombin addition show a more uniform network (Figure 4B,D). We also observed focal density (arrows in Figure 4A-B) where individual platelets concentrated the surrounding
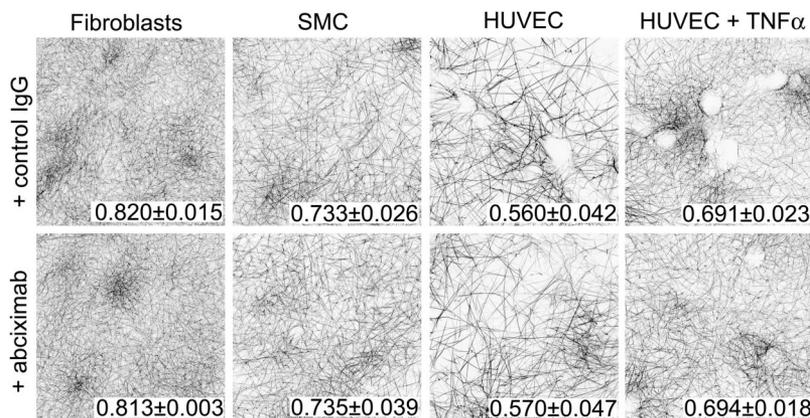

Figure 3. β 3 integrins do not modulate fibrin structure on fibroblasts, SMCs, or HUVECs. In situ thrombin generation was initiated by incubating fibroblasts, SMCs, and HUVECs with recalcified, normal, pooled PFP in the presence of 0.136μM control IgG or anti-β3 antibody (abciximab) as described in "Methods." Three-dimensional projections show clot architecture in 10-μm stacks 0 to 10 μm from the cell surface. Each image (146 μm × 146 μm, xy) is from 1 experiment, representative of 2 to 5 separate experiments. Data (no. fibers/point, ± SD) indicate mean fibrin network density from all experiments. Fibrin density in clots formed in the presence of control IgG or abciximab was not statistically different.
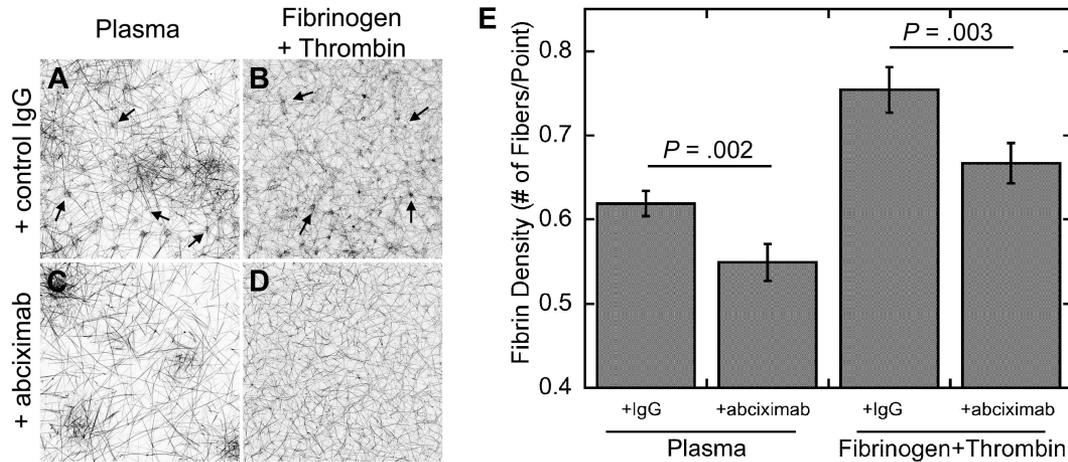
Figure 4. β 3 integrins modulate fibrin structure on platelets. (A,C) Clotting was initiated on platelets with the addition of recalcified, normal, pooled PFP to lipidated TF (1:120 000, final), in the presence of 0.136μM control IgG (A) or the anti-b3 Fab abciximab (C). (B,D) Clotting was initiated on platelets with the addition of fibrinogen, calcium, and thrombin (2 mg/mL, 5mM, and 2nM, respectively), in the presence of 0.136μM control IgG (B) or abciximab (D). Three-dimensional projections (146 μm × 146 μm, xy) show clot architecture in 10-μm stacks at 0 to 10 μm from the cell surface. Each image is from 1 experiment, representative of 4 independent experiments. Darker areas show increased fibrin density. Arrows in panels A and B indicate increased fibrin density surrounding individual platelets. (E) Data (± SD) indicate mean fibrin network density from all experiments. *$P < .004$ versus corresponding control IgG

fibrin network density in clots produced during in situ thrombin generation or exogenous thrombin addition. In contrast to findings on fibroblasts, SMCs, and HUVECs, abciximab significantly reduced fibrin density (larger patches and focal density) in clots produced by platelets during in situ thrombin generation, as well as during exogenous thrombin addition (Figure 4E). The effect of abciximab demonstrates the significant influence of platelet β3 integrin interactions on network density, likely reflecting the high concentration of β3 integrin subunits on platelets.[31] Together, these findings suggest the mechanism(s) dictating fibrin network structure on fibroblasts, SMCs, and HUVECs differs from those on platelets. Specifically, αIIbβ3 dictates network structure in platelet-rich clots, whereas integrin interactions play a minor to no role in clots formed by fibroblasts, SMCs, and HUVECs.

Fibrin produced by extravascular cells and TNFα-stimulated endothelial cells is more stable than that produced by unstimulated endothelial cells

Cellular procoagulant activity and fibrin network structure dictate clot fibrinolytic stability.[4,5,9] To compare lysis of clots produced by extravascular and intravascular cells, we added tPA (250 ng/mL,

final) to recalcified normal PFP, incubated the tPA-treated PFP with cells, and monitored fibrin formation and lysis by a turbidity increase and subsequent decrease, respectively, at 405 nm.[4] Traditional measures of fibrinolysis ("lysis time"—the time between the midpoints of the increase and decrease in turbidity[1] and "1/2 lysis time"—the time the turbidity drops to one-half the maximum turbidity[36,37]) are performed using a constant type and concentration of trigger to initiate clotting (thrombin or TF). However, because our experiments were initiated by cells expressing different TF concentrations, these lysis times were affected by the initiation of thrombin generation and subsequent effects on the lag times and rates of clot formation, limiting the utility of the traditional lysis measures. Therefore, we used the time to peak turbidity and the peak turbidity as measures of the time to maximum fibrin formation and the peak incorporation of fibrin into clot, respectively.[4] The ability of cellular procoagulant activity to increase fibrin stability shortens the time to peak and increases the peak turbidity. In these assays, fibroblasts and SMCs supported rapid formation of clots with high peak turbidity, whereas HUVECs produced the longest time to peak and lowest peak turbidity (Figure 5). Clots produced by TNFα-stimulated HUVECs exhibited a
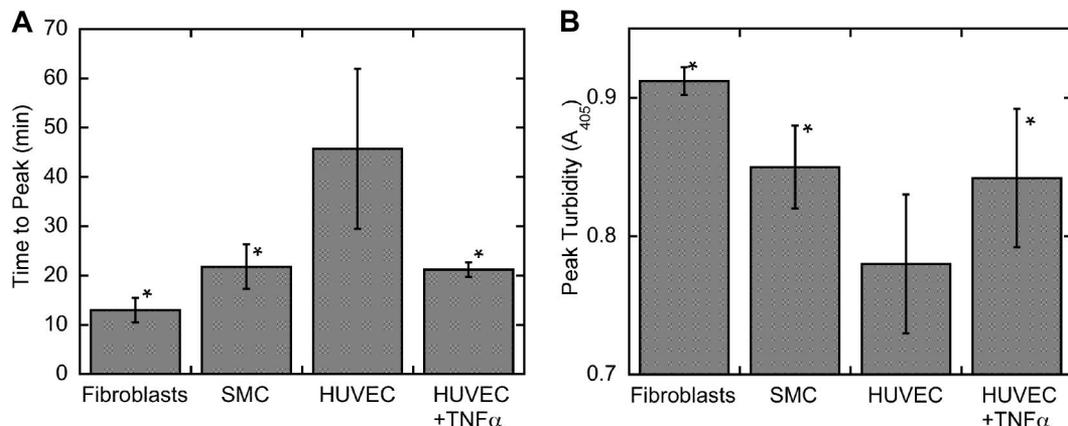

Figure 5. In situ thrombin generation influences clot stability. Clots were formed by incubating cells with recalcified normal, pooled PFP in the presence of tPA (250 ng/mL) and clot formation and lysis were monitored by an increase and subsequent decrease in turbidity at 405 nm. All values for (A) time to peak and (B) peak turbidity (± SD) were statistically different (*$P < .05$) compared with HUVECs.
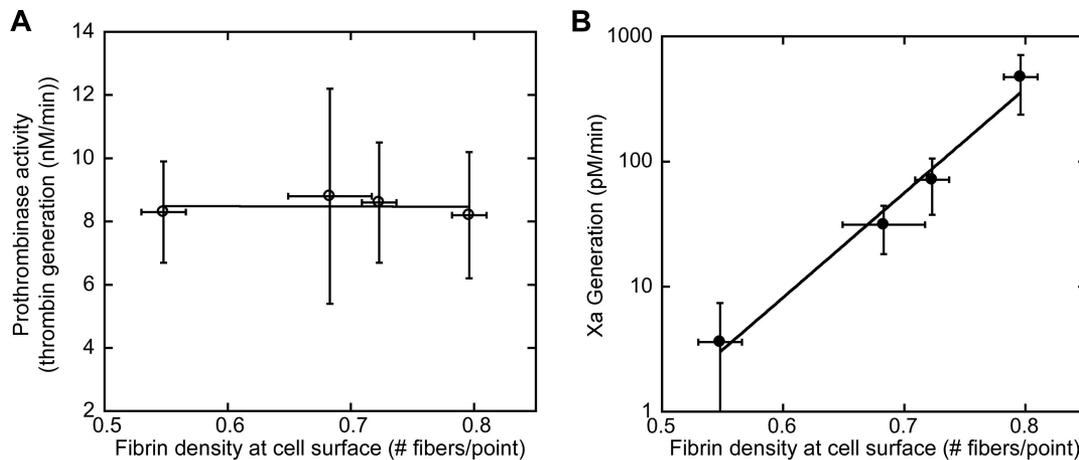
Figure 6. Fibrin network density correlates with cellular expression of TF activity. Factor Xa generation (○, A), prothrombinase activity (●, B), and fibrin density (x-axis) were measured in reactions with HUVECs, SMCs, TNFα-stimulated HUVECs, and fibroblasts (left to right) as described in "TF, prothrombinase activity, and activated protein C generation assays."

faster time to peak and higher peak turbidity than unstimulated HUVECs (Figure 5). In contrast, no differences in time to peak or peak turbidity were observed in plasma clots produced by exogenous thrombin addition (10nM) to these cells (data not shown), indicating the observed differences were due to cellular procoagulant activity and not cellular fibrinolytic or antifibrinolytic activities. Together, these findings suggest extravascular cells and TNFα-stimulated HUVECs produce stable networks that resist lysis, whereas unstimulated HUVECs produce less fibrin accumulation.

Fibrin network density correlates with cellular expression of TF activity

Our findings indicated that coagulant activity, and not integrins, dictated fibrin structure and stability. To probe the coagulant mechanism by which these cells dictate fibrin structure and stability, we characterized their specific procoagulant and anticoagulant activities. Fibroblasts, SMCs, and unstimulated and TNFα-stimulated HUVECs had similar prothrombinase activities, suggesting procoagulant phospholipid exposure was similar on each cell type (Figure 6A, Table 3). Consistent with previous studies,[38,39] SMCs, unstimulated HUVECs, and TNFα-stimulated HUVECs expressed thrombomodulin antigen (data not shown) and supported similar rates of protein C generation, whereas fibroblasts did not express thrombomodulin and supported significantly lower protein C generation (Table 3). Because fibroblasts, SMCs, and HUVECs produced clots with significantly different fibrin densities, these findings suggested neither prothrombinase activity nor activated protein C generation specifically dictated fibrin formation, structure, and/or stability on these cell types.

We then measured TF activity on these cells. Consistent with previous studies,[15,29] fibroblasts and SMCs supported 131-fold and 8.7-fold higher rates of factor Xa generation, respectively, than HUVECs (Table 3). Stimulating HUVECs for 4 hours with 1nM TNFα increased factor Xa generation 19.7-fold (Table 3). Anti-TF antibody (10 μg/mL, final) significantly reduced TF activity by 78%, 65%, and 85% on fibroblasts, SMCs, and TNFα-stimulated HUVECs, respectively (Table 3). Because the anti-TF antibody and recombinant factor VIIa (rFVIIa) were added to reactions simultaneously, competition between rFVIIa and anti-TF antibody for binding to TF prevented complete inhibition of TF activity. Together, these data showed a positive relationship between TF activity (Xa generation) and fibrin network density on these cells (Figure 6B), suggesting TF activity was the dominant mechanism differentiating procoagulant activity and subsequent fibrin network density of clots produced by these cells.

Reducing TF activity on stimulated HUVECs reduces fibrin clot density

Previous studies suggested TF inhibitors, including antibodies against TF[40] and active-site inhibited FVIIa,[41] reduce thrombus propagation and thrombus weight in animal models of thrombosis. Given the positive correlation between TF activity and fibrin network density, we hypothesized that TF and network structure are important targets for antithrombotic agents.

To determine whether TF inhibition alters fibrin structure and stability, we treated unstimulated and TNFα-stimulated HUVECs with anti-TF[42] or control IgG (10 μg/mL, final) and measured

Table 3. Procoagulant and anticoagulant properties of fibroblasts, SMCs, HUVECs, and TNFα-stimulated HUVECs

			HUVECs	
	Fibroblasts	**SMCs**	**Unstimulated**	**+ TNFα**
Prothrombinase activity, nM/min	8.2 ± 2.0	8.8 ± 3.4	8.3 ± 1.6	8.6 ± 1.9
Activated protein C, pM/min	18.6 ± 13.5*	45.3 ± 35.1	55.0 ± 29.2	57.9 ± 12.9
TF activity, pM/min				
− Anti-TF	475.0 ± 238.0*	31.3 ± 13.1*	3.6 ± 3.8	71.6 ± 34.0*
+ Anti-TF	109.0 ± 84.8*	11.0 ± 7.3*	3.6 ± 3.7	11.0 ± 7.3*

SMC indicates smooth muscle cell; HUVEC, human umbilical vein endothelial cell; TNFα, tumor necrosis factor-α; and TF, tissue factor.
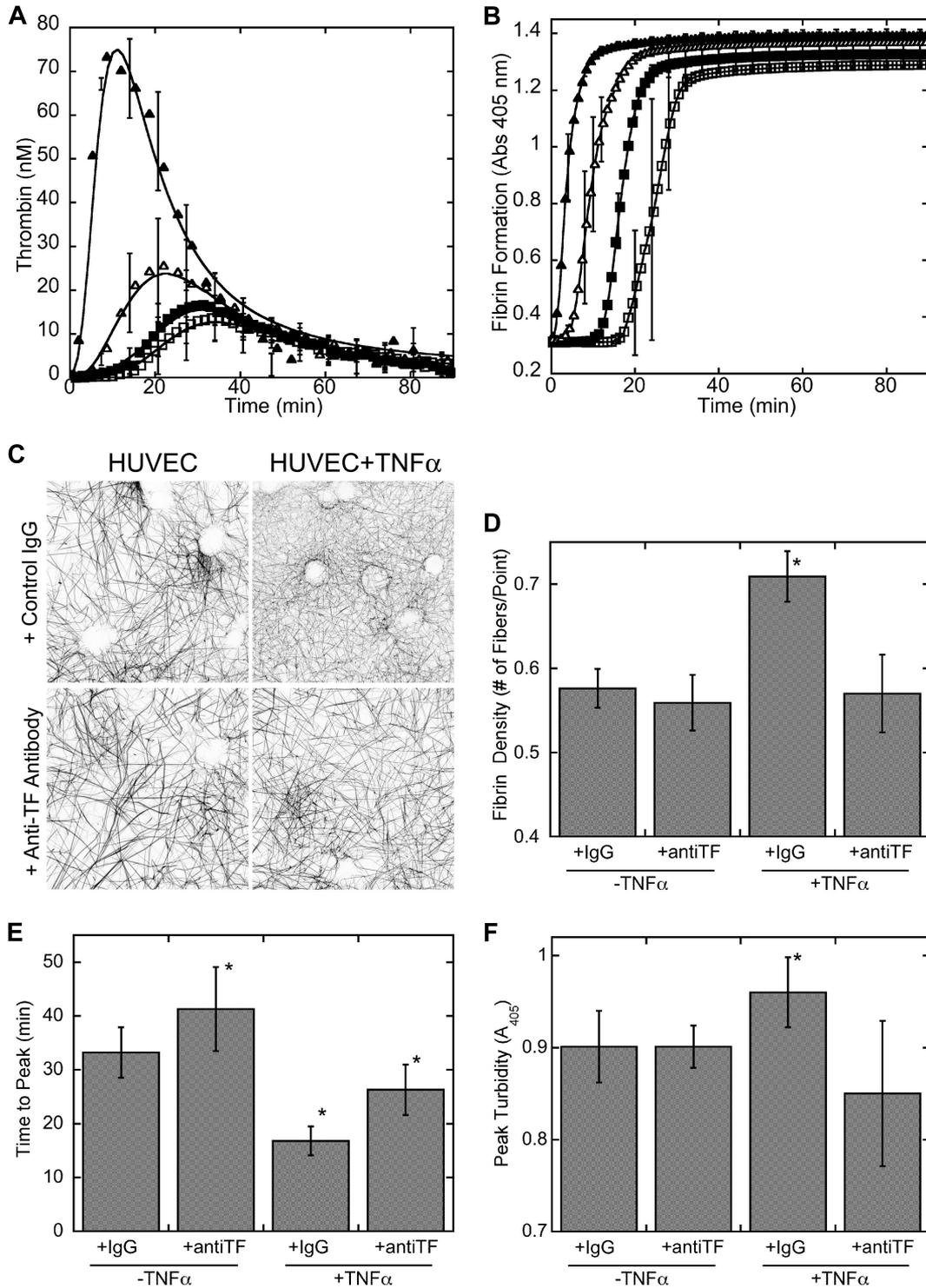
*P value less than .05 versus HUVECs.

Figure 7. TF inhibition prolongs the onset and reduces the rate of thrombin generation and clot formation, resulting in a less dense fibrin network. Recalcified (10mM, final) normal pooled PFP was added to confluent HUVECs and TNFα-treated HUVEC monolayers in the presence of anti-TF antibody (10 μg/mL anti–human TF antibody) or IgG control. (A) Thrombin generation was measured by calibrated automated thrombography. Data (± SD) show the average of 5 separate experiments. (B) Fibrin polymerization was monitored by turbidity at 405 nm. Data (± SD) shown are from 1 experiment, representative of 4 separate experiments. Symbols for panels A and B are HUVECs plus: IgG, (■); anti-TF, (□); TNFα+IgG, (▲); TNFα+anti-TF, (△). (C) Three-dimensional projections (146 μm × 146 μm, xy) show clot architecture in 10-μm stacks 0 to 10 μm from the surface of unstimulated or TNFα-stimulated HUVECs in the presence or absence of anti-TF, as indicated. Each image is from 1 experiment, representative of 4 independent experiments. (D) Fibrin density (± SD) was measured as described in "Methods." (E-F) Clotting was initiated in the presence of tPA (250 ng/mL) and the time to peak and peak turbidity were calculated from resulting turbidity curves. Data (± SD) show the average of 9 independent experiments. *$P < .05$ versus unstimulated HUVECs.

thrombin generation and fibrin formation and structure. On unstimulated HUVECs, addition of anti-TF antibody slightly and nonsignificantly prolonged the lag time of thrombin generation (Figure 7A) and onset of clot formation (Figure 7B), suggesting these unstimu-

lated, cultured cells express a low level of TF activity, likely due to their extraction from their native environment under shear. As in Figure 1B, the final turbidities of clots produced by these cells did not differ (Figure 7B) despite the substantial differences in cellular

procoagulant activity (Figure 7A). Addition of anti-TF to unstimulated HUVECs did not affect fibrin network structure (Figure 7C-D). However, addition of anti-TF antibody to TNFα-stimulated HUVECs significantly ($P < .05$) delayed the onset and decreased the peak height and time to peak thrombin generation (Figure 7A), prolonged the onset of clot formation (Figure 7B), and reduced the fibrin network density to levels found in clots produced by unstimulated HUVECs (Figure 7C-D). In the presence of tPA, anti-TF antibody prolonged the time to peak turbidity in clots produced by TNFα-stimulated HUVECs (Figure 7E). Importantly, the peak turbidity (fibrin incorporation) produced by TNFα-stimulated HUVECs in the presence of anti-TF was statistically indistinguishable from that produced by unstimulated HUVECs (Figure 7F). These findings suggest inhibiting thrombin generation, either through TF, Xa, or direct thrombin blockade, would significantly reduce fibrin formation and stability.

Discussion

A growing body of work has implicated fibrin structure and stability as important determinants of hemostasis and thrombosis. Most studies have focused on plasma contributions to clotting, showing that plasma clots from patients with bleeding disorders are composed of an abnormally coarse, unstable fibrin network, whereas plasma clots from patients with a personal or family history of thrombosis have an abnormally dense network that resists fibrinolysis.[1,2,43] Few studies have examined cellular contributions to clot structure and stability. In the current study, we showed that extravascular and intravascular cells support fibrin formation, structure, and stability. Our findings show extravascular cells supported the formation of a dense fibrin network that resisted fibrinolysis. Cytokine-stimulated intravascular cells similarly produced an abnormally dense, stable fibrin network that was inhibited by TF blockade. These findings suggest specific mechanisms by which different vascular cells contribute to hemostatic and thrombotic clot formation.

All of the examined cell types produced a denser fibrin network proximal to the cell surface compared with distal regions of the clot, consistent with our previous findings that thrombin generation on a fibroblast surface dictates the 3-dimensional network structure.[9] The current study extends the generality of this observation to 3 additional cell types (SMCs, HUVECs, and platelets) as well as cells lining freshly excised human saphenous veins. Experiments with excised saphenous veins in particular (Figure 2N) confirm the observation is not restricted to cultured cells, but is likely to arise from procoagulant activity of intravascular cells in vivo. Although a previous study showed the αv and β3 integrins significantly increase fibrin organization in clots produced on HUVECs,[32] we were unable to confirm this finding. Rather, we found in situ thrombin generation was both necessary and sufficient to increase fibrin density in clots produced by HUVECs, without further effect of cellular receptors. Differences between our findings and the previous work[32] may reflect differences in the source of HUVECs used in the study; the previous study used HUVECs from individual donors, whereas we used HUVECs pooled from 3 donors. We note, however, that although integrins did not significantly modulate fibrin structure of clots formed by TF-bearing cells, these findings do not preclude a role for cellular integrins in anchoring the fibrin network to the vessel wall. Further investigations of how clots anchor to surrounding cells are necessary to elucidate mechanisms that predispose some thrombi to embolism.

It is interesting that differences in fibrin structure seen by microscopy were not reflected in the final turbidity measurements of these clots (Figures 1B, 7B). In prior studies, turbidity and fibrin structure were studied using homogeneous fibrin networks. Our data suggest the fibrin structural gradient produced during in situ thrombin generation uncouples these measurements. These findings suggest studies performed in the presence of cells should include a microscopic method to directly visualize the fibrin network and validate turbidity measurements.

Fibroblasts and SMCs, present in the outmost and medial layers of the vessel wall, respectively, supported robust thrombin generation and clot formation, and produced dense, stable fibrin networks. After vascular breach, exposure of these cells to blood would initiate a rapid procoagulant response. In contrast, intravascular (endothelial) cells are specifically designed to prevent thrombin generation and fibrin production. The unstimulated HUVECs used in our study supported low thrombin generation and only coarse network formation. This basal activity of cultured endothelial cells probably reflects phenotypic changes upon removal of these cells from their native environment under flow.[44] Regardless, the observed differences between fibrin networks formed by endothelial cells and extravascular cells are profound, and suggest exposure of extravascular cells to blood would promote a stable fibrin network after vascular injury.

In atherosclerotic disease, exposure of blood to collagen and subendothelial cells (eg, SMCs) upon plaque rupture would be expected to produce a thrombus composed primarily of platelets and reinforced by a dense, overly stable fibrin network. Fibrin-rich venous clots, conversely, are thought to arise on intact endothelium.[45,46] In this case, exposure of intravascular cells to inflammatory mediators, including bacterial lipopolysaccharide,[16] hypoxia,[17] or cytokines,[18] may induce inappropriate intravascular TF expression. In our study, stimulating endothelial cells with TNFα increased TF expression and thrombin generation and caused the formation of dense fibrin networks, similar to those produced by extravascular cells (SMCs). We observed similar effects after treatment with IL-1β (data not shown), indicative of a generalized mechanism by which inflammatory mediators trigger a procoagulant/prothrombotic phenotype and subsequent intravascular fibrin formation.

It is interesting to note the difference in mechanisms dictating fibrin structure in clots produced by TF-bearing cells (procoagulant activity) and platelets (β3 integrin–fibrin interactions). Smyth et al[47] previously showed variable protection of β3-deficient mice from thrombosis initiated by different mechanisms. Whereas β3-deficient mice showed reduced thrombus formation in a model of arterial (platelet-rich) thrombosis, the β3-deficient mice were only minimally protected from TF-initiated microvascular thrombosis.[47] Our findings, consistent with these in vivo thrombosis models, provide a mechanistic basis for the effectiveness of β3-blocking strategies in preventing platelet-rich arterial thrombi[48] versus anticoagulants to prevent fibrin-rich venous thrombi.[49,50]

Our findings show a crucial role for TF activity in fibrin network formation, structure, and stability. Compared with unstimulated HUVECs, TNFα-stimulated HUVECs expressed significantly higher TF activity, but similar lipid and thrombomodulin expression. Thus, increased TF activity alone was sufficient to increase thrombin generation and fibrin density to levels seen in clots produced by extravascular SMCs. Blocking TF activity on TNFα-stimulated endothelial cells reduced procoagulant activity and fibrin density and stability to that of unstimulated cells, lending

support to a mechanism by which VIIa/TF inhibition reduces venous thrombosis.[40]

Our current experimental design omits the effects of shear on fibrin formation, structure, and stability. Previous studies have demonstrated that endothelial cells are less susceptible to TNFα-induced TF expression in the presence of shear.[51] However, once stimulated, endothelial cells support robust thrombin and fibrin formation under low shear, whereas high shear suppresses fibrin deposition.[52] Interestingly, higher TF concentrations increase the shear threshold that attenuates fibrin production.[53] Together, these studies suggest that reduced shear (stasis) promotes endothelial cell susceptibility to cytokine stimulation, and that the combination of activated endothelial cells and low shear promotes local thrombus formation. Although the previous studies examined the role of shear and TF concentration on fibrin deposition,[53,54] the resulting fibrin structures were not evaluated. Based on our current study, evaluating fibrin structure under different shear forces may offer insight into the role of stasis in thrombus formation.

Our results provide an important foundation for future studies of cell types from different vascular beds. Our system allows for the examination of how cellular properties such as TF[55] and thrombin[13] expression on endothelial cells from the arterial, venous, and microvascular circulation, or binding of TF microparticles,[56] contribute to clot structure and stability. Such studies are critical for understanding the role of the endothelium in vascular bed–specific thrombosis. Furthermore, our system enables the examination of how interactions between soluble clotting factors and vascular cells promote clot formation. Effects of hypercoagulability and endothelial dysfunction may be additive or even synergistic with regard to thrombin generation and fibrin production. Studies on the combined effects of these cellular and plasma activities remain interesting next steps in these investigations.

Authorship

Contribution: R.A.C. designed and performed the experiments, analyzed and interpreted the data, and wrote the manuscript; K.A.O. designed and performed the experiments, and analyzed and interpreted the data; C.H.S. and B.C.S. contributed vital reagents; and A.S.W. designed the research, analyzed and interpreted data, and wrote the manuscript.

Conflict-of-interest disclosure: A.S.W. received research funding from Novo Nordisk. The remaining authors declare no competing financial interests.

R.A.C.'s current affiliation is Department of Human Molecular Biology and Genetics, University of Utah, Salt Lake City. K.A.O.'s current affiliation is Department of Molecular and Integrative Physiology, University of Michigan, Ann Arbor. C.H.S.'s current affiliation is Division of Cardiothoracic Surgery, Department of Surgery, University of Utah, Salt Lake City.

Correspondence: Alisa S. Wolberg, Department of Pathology and Laboratory Medicine, University of North Carolina at Chapel Hill, 815 Brinkhous-Bullitt Bldg, CB #7525, Chapel Hill, NC 27599-7525; e-mail: alisa_wolberg@med.unc.edu.

References

1. Lisman T, de Groot PG, Meijers JC, Rosendaal FR. Reduced plasma fibrinolytic potential is a risk factor for venous thrombosis. *Blood.* 2005;105(3):1102-1105.

2. Collet JP, Allali Y, Lesty C, et al. Altered fibrin architecture is associated with hypofibrinolysis and premature coronary atherothrombosis. *Arterioscler Thromb Vasc Biol.* 2006;26(11):2567-2573.

3. Blombäck B, Carlsson K, Hessel B, Liljeborg A, Procyk R, Aslund N. Native fibrin gel networks observed by 3D microscopy, permeation and turbidity. *Biochim Biophys Acta.* 1989;997(1-2):96-110.

4. Wolberg AS, Allen GA, Monroe DM, Hedner U, Roberts HR, Hoffman M. High dose factor VIIa improves clot structure and stability in a model of haemophilia B. *Br J Haematol.* 2005;131(5):645-655.

5. Collet JP, Park D, Lesty C, et al. Influence of fibrin network conformation and fibrin fiber diameter on fibrinolysis speed: dynamic and structural approaches by confocal microscopy. *Arterioscler Thromb Vasc Biol.* 2000;20(5):1354-1361.

6. Carr ME Jr, Alving BM. Effect of fibrin structure on plasmin-mediated dissolution of plasma clots. *Blood Coagul Fibrinolysis.* 1995;6(6):567-573.

7. Smith SA, Morrissey JH. Polyphosphate enhances fibrin clot structure. *Blood.* 2008;112(7):2810-2816.

8. Mosnier LO, von dem Borne PA, Meijers JC, Bouma BN. Plasma TAFI levels influence the clot lysis time in healthy individuals in the presence of an intact intrinsic pathway of coagulation. *Thromb Haemost.* 1998;80(5):829-835.

9. Campbell RA, Overmyer KA, Bagnell CR, Wolberg AS. Cellular procoagulant activity dictates clot structure and stability as a function of distance from the cell surface. *Arterioscler Thromb Vasc Biol.* 2008;28(12):2247-2254.

10. Subbaiah PV, Bajwa SS, Smith CM, Hanahan DJ. Interactions of the components of the prothrombinase complex. *Biochim Biophys Acta.* 1976;444(1):131-146.

11. Broze GJ Jr, Warren LA, Novotny WF, Higuchi DA, Girard JJ, Miletich JP. The lipoprotein-associated coagulation inhibitor that inhibits the factor VII-tissue factor complex also inhibits factor Xa: insight into its possible mechanism of action. *Blood.* 1988;71(2):335-343.

12. Stearns-Kurosawa DJ, Kurosawa S, Mollica JS, Ferrell GL, Esmon CT. The endothelial cell protein C receptor augments protein C activation by the thrombin-thrombomodulin complex. *Proc Natl Acad Sci U S A.* 1996;93(19):10212-10216.

13. Aird WC. Vascular bed-specific thrombosis. *J Thromb Haemost.* 2007;5(suppl 1):283-291.

14. Rodgers GM, Greenberg CS, Shuman MA. Characterization of the effects of cultured vascular cells on the activation of blood coagulation. *Blood.* 1983;61(6):1155-1162.

15. Ovanesov MV, Ananyeva NM, Panteleev MA, Ataullakhanov FI, Saenko EL. Initiation and propagation of coagulation from tissue factor-bearing cell monolayers to plasma: initiator cells do not regulate spatial growth rate. *J Thromb Haemost.* 2005;3(2):321-331.

16. Noguchi M, Sakai T, Kisiel W. Correlation between antigenic and functional expression of tissue factor on the surface of cultured human endothelial cells following stimulation by lipopolysaccharide endotoxin. *Thromb Res.* 1989;55(1):87-97.

17. Ogawa S, Gerlach H, Esposito C, Pasagian-Macaulay A, Brett J, Stern D. Hypoxia modulates the barrier and coagulant function of cultured bovine endothelium: increased monolayer permeability and induction of procoagulant properties. *J Clin Invest.* 1990;85(4):1090-1098.

18. Bevilacqua MP, Pober JS, Majeau GR, Fiers W, Cotran RS, Gimbrone MA Jr. Recombinant tumor necrosis factor induces procoagulant activity in cultured human vascular endothelium: characterization and comparison with the actions of interleukin 1. *Proc Natl Acad Sci U S A.* 1986;83(12):4533-4537.

19. Heffernan TP, Simpson DA, Frank AR, et al. An ATR- and Chk1-dependent S checkpoint inhibits replicon initiation following UVC-induced DNA damage. *Mol Cell Biol.* 2002;22(24):8552-8561.

20. Wolberg AS, Monroe DM, Roberts HR, Hoffman MR. Tissue factor de-encryption: ionophore treatment induces changes in tissue factor activity by phosphatidylserine-dependent and -independent mechanisms. *Blood Coagul Fibrinolysis.* 1999;10(4):201-210.

21. Nan B, Lin P, Lumsden AB, Yao Q, Chen C. Effects of TNF-alpha and curcumin on the expression of thrombomodulin and endothelial protein C receptor in human endothelial cells. *Thromb Res.* 2005;115(5):417-426.

22. Luddington R, Baglin T. Clinical measurement of thrombin generation by calibrated automated thrombography requires contact factor inhibition. *J Thromb Haemost.* 2004;2(11):1954-1959.

23. Hemker HC, Giesen P, Al Dieri R, et al. Calibrated automated thrombin generation measurement in clotting plasma. *Pathophysiol Haemost Thromb.* 2003;33(1):4-15.

24. Ollivier V, Wang J, Manly D, et al. Detection of endogenous tissue factor levels in plasma using the calibrated automated thrombogram assay. *Thromb Res.* Apr 3 2009. [Epub ahead of print]

25. Machlus KR, Colby EA, Wu JR, Koch GG, Key NS, Wolberg AS. Effects of tissue factor, thrombomodulin, and elevated clotting factor levels on thrombin generation in the calibrated automated thrombogram. *Thromb Haemost.* 2009;102(5):936-944.

26. Galdal KS, Evensen SA, Hoglund AS, Nilsen E. Actin pools and actin microfilament organization in cultured human endothelial cells after exposure to thrombin. *Br J Haematol.* 1984;58(4):617-625.

27. Dorsam RT, Kim S, Jin J, Kunapuli SP. Coordinated signaling through both G12/13 and G(i) pathways is sufficient to activate GPIIb/IIIa in human platelets. *J Biol Chem.* 2002;277(49):47588-47595.

28. Hoffman M, Monroe DM, Roberts HR. A rapid method to isolate platelets from human blood by density gradient centrifugation. *Am J Clin Pathol.* 1992;98(5):531-533.

29. Zwaginga JJ, de Boer HC, MJ IJ, et al. Thrombogenicity of vascular cells. Comparison between endothelial cells isolated from different sources and smooth muscle cells and fibroblasts. *Arteriosclerosis.* 1990;10(3):437-448.

30. Herbert JM, Savi P, Laplace MC, Lale A. IL-4 inhibits LPS-, IL-1 beta- and TNF alpha-induced expression of tissue factor in endothelial cells and monocytes. *FEBS Lett.* 1992;310(1):31-33.

31. Collet JP, Montalescot G, Lesty C, et al. Disaggregation of in vitro preformed platelet-rich clots by abciximab increases fibrin exposure and promotes fibrinolysis. *Arterioscler Thromb Vasc Biol.* 2001;21(1):142-148.

32. Jerome WG, Handt S, Hantgan RR. Endothelial cells organize fibrin clots into structures that are more resistant to lysis. *Microsc Microanal.* 2005;11(3):268-277.

33. Chang MC, Wang BR, Huang TF. Characterization of endothelial cell differential attachment to fibrin and fibrinogen and its inhibition by Arg-Gly-Asp-containing peptides. *Thromb Haemost.* 1995;74(2):764-769.

34. Yee KO, Rooney MM, Giachelli CM, Lord ST, Schwartz SM. Role of beta1 and beta3 integrins in human smooth muscle cell adhesion to and contraction of fibrin clots in vitro. *Circ Res.* 1998;83(3):241-251.

35. Farrell DH, al-Mondhiry HA. Human fibroblast adhesion to fibrinogen. *Biochemistry.* 1997;36(5):1123-1128.

36. Pandi L, Kollman JM, Lopez-Lira F, Burrows JM, Riley M, Doolittle RF. Two families of synthetic peptides that enhance fibrin turbidity and delay fibrinolysis by different mechanisms. *Biochemistry.* 2009;48(30):7201-7208.

37. Doolittle RF, Pandi L. Probing the beta-chain hole of fibrinogen with synthetic peptides that differ at their amino termini. *Biochemistry.* 2007;46(35):10033-10038.

38. Esmon CT, Owen WG. Identification of an endothelial cell cofactor for thrombin-catalyzed activation of protein C. *Proc Natl Acad Sci U S A.* 1981;78(4):2249-2252.

39. Soff GA, Jackman RW, Rosenberg RD. Expression of thrombomodulin by smooth muscle cells in culture: different effects of tumor necrosis factor and cyclic adenosine monophosphate on thrombomodulin expression by endothelial cells and smooth muscle cells in culture. *Blood.* 1991;77(3):515-518.

40. Himber J, Wohlgensinger C, Roux S, et al. Inhibition of tissue factor limits the growth of venous thrombus in the rabbit. *J Thromb Haemost.* 2003;1(5):889-895.

41. Holst J, Kristensen AT, Kristensen HI, Ezban M, Hedner U. Local application of recombinant active-site inhibited human clotting factor VIIa reduces thrombus weight and improves patency in a rabbit venous thrombosis model. *Eur J Vasc Endovasc Surg.* 1998;15(6):515-520.

42. Carson SD, Ross SE, Bach R, Guha A. An inhibitory monoclonal antibody against human tissue factor. *Blood.* 1987;70(2):490-493.

43. Wolberg AS, Monroe DM, Roberts HR, Hoffman M. Elevated prothrombin results in clots with an altered fiber structure: a possible mechanism of the increased thrombotic risk. *Blood.* 2003;101(8):3008-3013.

44. Reverdiau P, Jarousseau AC, Thibault G, et al. Tissue factor activity of syncytiotrophoblast plasma membranes and tumoral trophoblast cells in culture. *Thromb Haemost.* 1995;73(1):49-54.

45. Sevitt S. The structure and growth of valve-pocket thrombi in femoral veins. *J Clin Pathol.* 1974;27(7):517-528.

46. Day TK, Cowper SV, Kakkar VV, Clark KG. Early venous thrombosis: A scanning electron microscopic study. *Thromb Haemost.* 1977;37(3):477-483.

47. Smyth SS, Reis ED, Vaananen H, Zhang W, Coller BS. Variable protection of beta 3-integrin–deficient mice from thrombosis initiated by different mechanisms. *Blood.* 2001;98(4):1055-1062.

48. Oster ZH, Srivastava SC, Som P, et al. Thrombus radioimmunoscintigraphy: an approach using monoclonal antiplatelet antibody. *Proc Natl Acad Sci U S A.* 1985;82(10):3465-3468.

49. Gent M, Hirsh J, Ginsberg JS, et al. Low-molecular-weight heparinoid orgaran is more effective than aspirin in the prevention of venous thromboembolism after surgery for hip fracture. *Circulation.* 1996;93(1):80-84.

50. Glynn RJ, Ridker PM, Goldhaber SZ, Buring JE. Effect of low-dose aspirin on the occurrence of venous thromboembolism: a randomized trial. *Ann Intern Med.* 2007;147(8):525-533.

51. Matsumoto Y, Kawai Y, Watanabe K, et al. Fluid shear stress attenuates tumor necrosis factor-alpha-induced tissue factor expression in cultured human endothelial cells. *Blood.* 1998;91(11):4164-4172.

52. Diquélou A, Dupouy D, Gaspin D, et al. Relationship between endothelial tissue factor and thrombogenesis under blood flow conditions. *Thromb Haemost.* 1995;74(2):778-783.

53. Runyon MK, Kastrup CJ, Johnson-Kerner BL, Ha TG, Ismagilov RF. Effects of shear rate on propagation of blood clotting determined using microfluidics and numerical simulations. *J Am Chem Soc.* 2008;130(11):3458-3464.

54. Okorie UM, Denney WS, Chatterjee MS, Neeves KB, Diamond SL. Determination of surface tissue factor thresholds that trigger coagulation at venous and arterial shear rates: amplification of 100 fM circulating tissue factor requires flow. *Blood.* 2008;111(7):3507-3513.

55. Day SM, Reeve JL, Pedersen B, et al. Macrovascular thrombosis is driven by tissue factor derived primarily from the blood vessel wall. *Blood.* 2005;105(1):192-198.

56. Sullivan VV, Hawley AE, Farris DM, et al. Decrease in fibrin content of venous thrombi in selectin-deficient mice. *J Surg Res.* 2003;109(1):1-7.